

Program “The Creation of Basic Medical Technologies to Clarify and Control the Mechanisms Underlying Chronic Inflammation” of Japan Science and Technology Agency (JST) to O.N., by a grant for HPIC STRATEGIC PROGRAM Computational Life Science and Application in Drug Discovery and Medical Development by MEXT to R.I., by a Grant-in-Aid for Scientific Research on Innovative Areas (23136517) from Ministry of Education, Culture, Sports, Science and Technology (MEXT) to S.K., by a Grant-in-Aid for Scientific Research (C) (23590319) from JSPS to T.I., and by a Grant-in-Aid for Scientific Research (S) (24227004) and a Grant-in-Aid for Young Scientists (A) (22687007) from the MEXT to O.N. and

R.I., respectively. T.N. expressed and purified CAX\_Af for crystallization, collected the diffraction data, solved the structures, and performed functional analyses in liposomes. N.F. screened CaCA genes and identified CAX\_Af. S.K. and T.I. performed transport assays in *E. coli* cells. A.D.M. performed transport assays in *E. coli* spheroplasts. G.K. made mutants. K.H. assisted with data collection. S.O. supported crystallization. N.D. analyzed the purified protein by mass spectrometry. T.N., R.I., and O.N. wrote the manuscript. R.I. and O.N. directed and supervised all of the research. The coordinates and the structure factors have been deposited in the Protein Data Bank (PDB) under accession codes 4KPP.

### Supplementary Materials

www.sciencemag.org/cgi/content/full/science.1239002/DC1  
Materials and Methods  
Supplementary Text  
Figs. S1 to S14  
Tables S1 to S2  
References (14–24)  
Movie S1

10 April 2013; accepted 15 May 2013

Published online 23 May 2013;  
10.1126/science.1239002

# Crystal Structure of NLRC4 Reveals Its Autoinhibition Mechanism

Zehan Hu,<sup>1,2,3</sup> Chuangye Yan,<sup>1</sup> Peiyuan Liu,<sup>1</sup> Zhiwei Huang,<sup>4</sup> Rui Ma,<sup>1</sup> Chenlu Zhang,<sup>1</sup> Ruiyong Wang,<sup>5</sup> Yueteng Zhang,<sup>5</sup> Fabio Martinon,<sup>6</sup> Di Miao,<sup>1</sup> Haiteng Deng,<sup>1</sup> Jiawei Wang,<sup>1</sup> Junbiao Chang,<sup>5</sup> Jijie Chai<sup>1\*</sup>

Nucleotide-binding and oligomerization domain–like receptor (NLR) proteins oligomerize into multiprotein complexes termed inflammasomes when activated. Their autoinhibition mechanism remains poorly defined. Here, we report the crystal structure of mouse NLRC4 in a closed form. The adenosine diphosphate–mediated interaction between the central nucleotide-binding domain (NBD) and the winged-helix domain (WHD) was critical for stabilizing the closed conformation of NLRC4. The helical domain HD2 repressively contacted a conserved and functionally important  $\alpha$ -helix of the NBD. The C-terminal leucine-rich repeat (LRR) domain is positioned to sterically occlude one side of the NBD domain and consequently sequester NLRC4 in a monomeric state. Disruption of ADP-mediated NBD–WHD or NBD–HD2/NBD–LRR interactions resulted in constitutive activation of NLRC4. Together, our data reveal the NBD-organized cooperative autoinhibition mechanism of NLRC4 and provide insight into its activation.

**N**ucleotide-binding and oligomerization domain (NOD)–like receptors (NLRs) constitute a crucial component of the cytosolic immunosurveillance system of mammals by detecting the signature components of pathogens and consequently triggering immune responses (1–4). Dysregulation of NLR function has been associated with a variety of diseases (5–7).

NLR proteins typically comprise a varied N-terminal effector domain, such as caspase-recruitment domain (CARD) or pyrin domain; a central NOD; and a C-terminal leucine-rich repeat (LRR) domain (1). NLRs belong to the signal transduction adenosine triphosphatases (ATPases) with numerous domains (STAND) subfamily, including Apaf-1 and CED-4 (8). The current model of NLR activation posits that ligand binding to the C-terminal LRR sensor domain results in exchange of adenosine diphosphate (ADP) for ATP followed by oligomerization (8). Indeed, ligand-induced oligomerization was shown for several NLR members, including NLRC4 (NLR

family CARD domain–containing protein 4) (9–14). Oligomerization results in the recruitment of signaling molecules, which together with NLRs,

make up the inflammasome, a multiprotein complex that triggers host innate immune responses and rapid cell death. The NLRC4 inflammasome is activated in mice by bacterial flagellin (14–19) or the components of type 3 secretion systems (14, 15, 19, 20).

In order to understand the structure of NLRC4, we made a mouse NLRC4 (mNLRC4) mutant with the CARD (residues 1 to 89) and the internal residues (622 to 644) deleted (mNLRC4 $\Delta$ CARD) (fig. S1). mNLRC4 with the latter deletion only was still functional (fig. S2). Similar to the full-length mNLRC4 protein and consistent with previous data (14), the mNLRC4 $\Delta$ CARD protein showed no defect in protein folding (fig. S3) and was monomeric in solution (fig. S4). The crystal structure of mNLRC4 $\Delta$ CARD was solved at a resolution of 3.2 Å (table S1 and fig. S5).

The overall structure of mNLRC4 $\Delta$ CARD is shaped like an inverted question mark (Fig. 1). The NOD module comprises the nucleotide-binding domain (NBD), the helical domain HD1, and the winged-helix domain (WHD). As observed in all

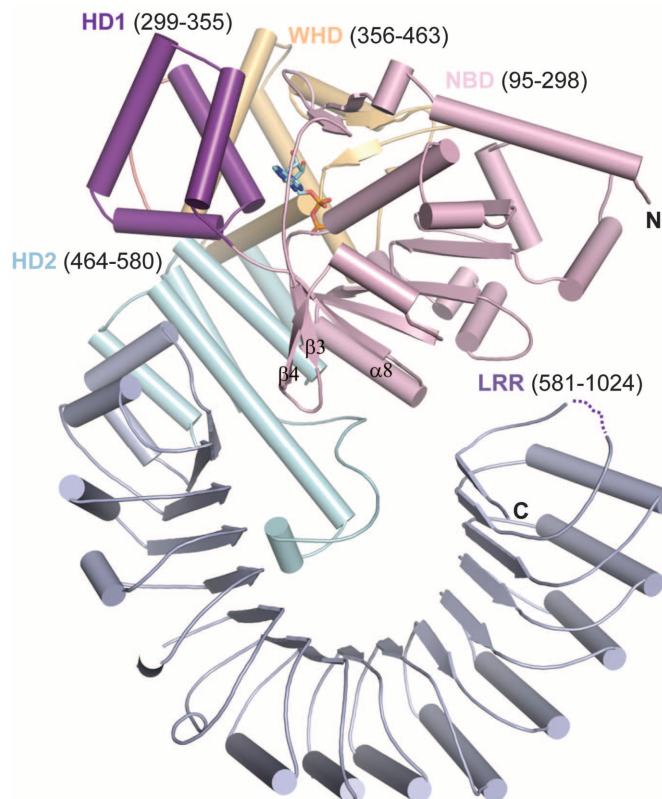


**Fig. 1. Overall structure of mNLRC4 $\Delta$ CARD.** The overall structure of mNLRC4 $\Delta$ CARD shown in cartoon. The structural domains of mNLRC4 $\Delta$ CARD are labeled, and the numbers following their labels indicate their boundaries. The bound ADP molecule is shown in stick and cyan. Some of the structural elements are labeled. The dashed line indicates the disordered region (residues 1011 to 1014). “N” and “C” represent N terminus and C terminus, respectively.

<sup>1</sup>School of Life Sciences, Tsinghua University, and Tsinghua-Peking Center for Life Sciences, Beijing 100084, China. <sup>2</sup>National Institute of Biological Sciences, Number 7 Science Park Road, Beijing 102206, China. <sup>3</sup>College of Life Sciences, Beijing Normal University, Beijing 100875, China. <sup>4</sup>School of Life Science and Biotechnology, Harbin Institute of Technology, Harbin 150080, China. <sup>5</sup>College of Chemistry and Molecular Engineering, Zhengzhou University, Zhengzhou 450001, China. <sup>6</sup>Department of Biochemistry, Lausanne University, 1066 Lausanne, Switzerland.

\*Corresponding author. E-mail:chaijj@mail.tsinghua.edu.cn

the other AAA+ ATPase structures (21), the NBD of mNLRC4 $\Delta$ CARD is a three-layered  $\alpha/\beta$  structure but possesses an additional  $\beta$  hairpin ( $\beta 3$  and  $\beta 4$ ) (Fig. 1). In vitro study showed that the

mNLRC4 protein was an active ATPase (fig. S6). Although not supplemented during the experiment, an ADP molecule was well defined by the electron density (fig. S7). The HD2 domain caps

the N-terminal side of the LRR domain via extensive interactions (fig. S8). The LRR domain is located distant from the HD1 and WHD domains and the ADP-binding site (Fig. 1). Its structural

**Fig. 2. Critical role of the ADP-mediated WHD-NBD interaction in mNLRC4 autoinhibition.**

(A) The ADP-bound mNLRC4 $\Delta$ CARD is in a closed conformation. Structural comparison of the NOD of mNLRC4 $\Delta$ CARD with that of the inactive Apaf-1 (PDB code 3SFZ). Color codes for domains of mNLRC4 $\Delta$ CARD and Apaf-1 are indicated. The bound ADPs (in stick) in mNLRC4 $\Delta$ CARD and in Apaf-1 are shown in cyan and yellow, respectively. (B) Recognition of ADP by mNLRC4. Detailed interactions of ADP with mNLRC4 from the area highlighted in (A). The dashed red lines indicate polar (hydrogen and salt) interactions. (C) Transfection of 293T cells with plasmids as indicated. A twofold serial dilution was made for the transfection of H443L. After 24 hours, the culture medium was supplemented with PA (protective antigen) and LFn (N-terminal domain of anthrax lethal factor)—FliC (C-terminal part of flagellin) proteins. The cells were lysed, and the cleaved IL-1 $\beta$  was detected by anti-IL-1 $\beta$  immunoblotting analysis after 12 hours.  $\beta$ -actin was used as a loading control. The experiments were repeated five times. WT, wild type; HA, hemagglutinin. (D) Transfection of 293T cells with plasmids as indicated. Thirty-six hours after the transfection, cells were lysed and subjected to gel-filtration chromatography. All the fractions were collected and detected by anti-Myc epitope immunoblotting analysis.

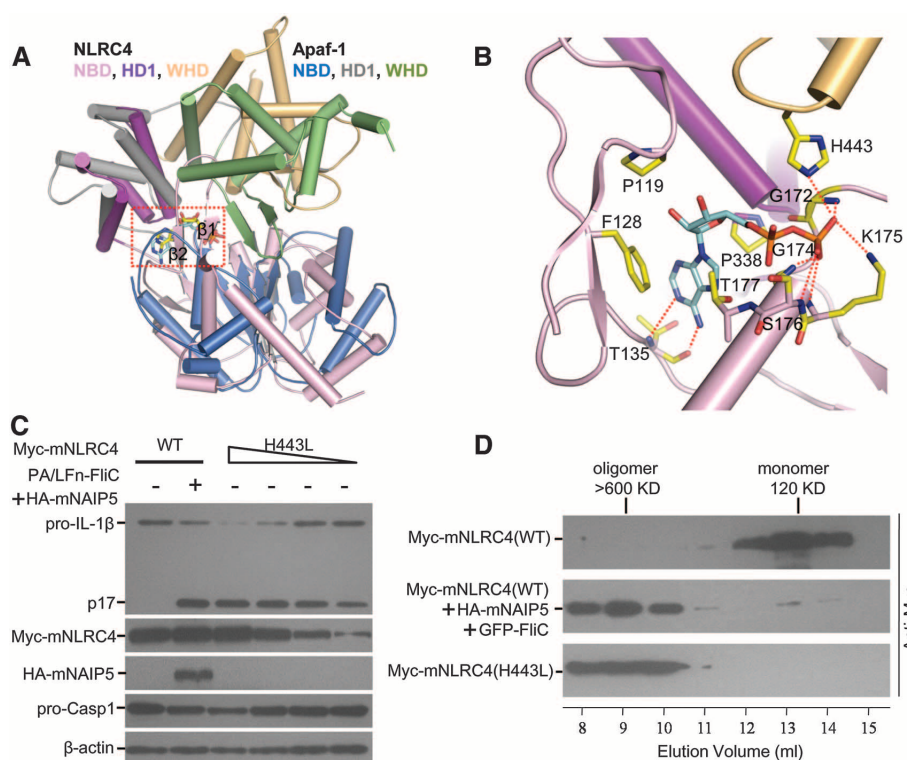
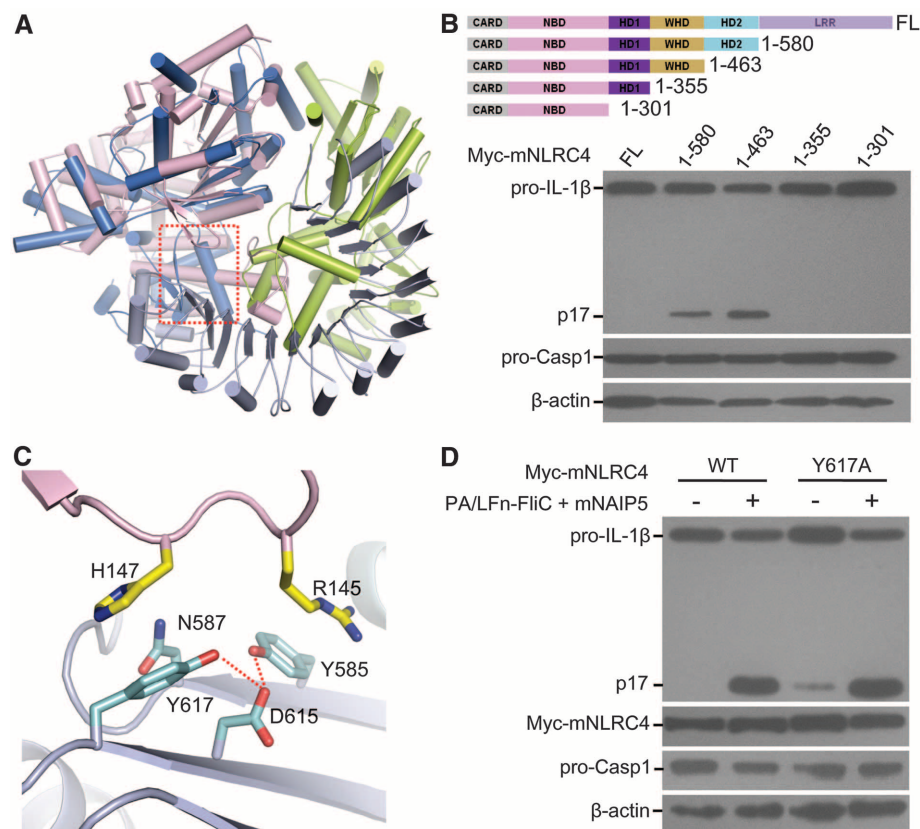


**Fig. 3. The C-terminal LRR domain sequesters mNLRC4 in a monomeric state.**

(A) The LRR domain of mNLRC4 $\Delta$ CARD overlaps with one protomer of CED-4 from a lateral dimer. Shown is the structural superposition of mNLRC4 $\Delta$ CARD with a lateral dimer of CED-4 (PDB code 3LQQ). The NOD of mNLRC4 $\Delta$ CARD was used as the template to superimpose with one protomer of a CED-4 lateral dimer. The LRR is shown in slate, the remaining part of mNLRC4 $\Delta$ CARD in pink, and the two CED-4 protomers in blue and green. (B) (Top) Schematic diagram of mNLRC4 truncation mutants. (Bottom) The assay was performed as described in Fig. 2C, and 293T cells were transfected with plasmids as indicated. The experiment was repeated three times. FL, full length. (C) Detailed LRR-NBD interactions from the area highlighted in (A). The side chains from NBD are shown in yellow and those from LRR in cyan. D, Asp; N, Asn. (D) Analysis of mutants disrupting LRR-NBD interactions. The assay was performed as described in Fig. 2C and repeated three times.



coupling with the NOD is established through the additional  $\beta$  hairpin (Fig. 1). Marginal NBD-LRR interactions results in closure of the solenoid structure.

A DALI search identified the NOD domains of Apaf-1 (22, 23) and CED-4 (24, 25) as the closest homologs to mNLRC4 $\Delta$ CARD (Fig. 2A and fig. S9). Compared with the closed form of Apaf-1, mNLRC4 $\Delta$ CARD possesses an extra  $\beta$  sheet ( $\beta 1$  and  $\beta 2$ ) that pushes the WHD away from the NBD (Fig. 2A). Nevertheless, the WHD of mNLRC4 $\Delta$ CARD still faces the front of the ADP binding site, indicating that the ADP-bound mNLRC4 $\Delta$ CARD adopts a closed conformation according to previous classification (8). This is in contrast with the WHD of CED-4 (25) (fig. S9A), although the structures of the three WHDs are well superimposed (fig. S10). ADP appears to be critical for locking mNLRC4 $\Delta$ CARD in an inactive conformation. The phosphate groups of ADP structure the Walker A motif (fig. S1), with five hydrogen bonds formed between them (Fig. 2B). Two additional hydrogen bonds between ADP and the NBD come from coordination of the N1 and N6 atoms in the adenine but not the guanine base with Thr<sup>135</sup>. Like His<sup>438</sup> in the inactive

Apaf-1, His<sup>443</sup> from the WHD of mNLRC4 $\Delta$ CARD also hydrogen bonds with the  $\beta$ -phosphate group of the ADP molecule (Fig. 2B).

The WHD of Apaf-1 undergoes notable structural remodeling with respect to its NBD after oligomerization (23, 26). This is also expected for the WHD of mNLRC4, given its similar positioning to inactive Apaf-1 (Fig. 2A). Thus, the interaction of His<sup>443</sup> with the  $\beta$ -phosphate group is likely specific for the ADP-bound mNLRC4. Disruption of the interaction would facilitate conformational changes in the WHD and attenuate ADP binding, both of which favor mNLRC4 activation. We, therefore, examined the activity of the mutant His<sup>443</sup>→Leu<sup>443</sup> (H443L) in processing interleukin (IL)-1 $\beta$  by using the assays established previously (14, 19). The mutant protein, even when expressed at a lower level than that of the wild-type mNLRC4, bypassed the requirement of flagellin and mouse NLR family, apoptosis inhibitory protein 5 (mNAIP5, which functions upstream of NLRC4) for IL-1 $\beta$  activation (Fig. 2C). Consistent with its constitutive activity, the mutant protein formed a higher order of oligomers when overexpressed in 293T cells (Fig. 2D).

Oligomerization of CED-4 (25), Apaf-1 (27), and the *Drosophila* Apaf-1 (DARK) (27) involves a conserved mode of domain organization: One side of the NBD from one protomer stacks against the opposite side of the NBD from the other protomer in a lateral dimer (fig. S11). Structural superposition of mNLRC4 $\Delta$ CARD with one protomer of a lateral CED-4 dimer (24) revealed that the LRR domain completely overlaps with the other CED-4 protomer (Fig. 3A), suggesting that the LRR has a role in sequestering mNLRC4 in a monomeric state. Indeed, the LRR deletion led to a constitutively active mNLRC4 in processing of IL-1 $\beta$  (Fig. 3B and fig. S12A), consistent with previous data (14). Further removal of the HD2 appeared to result in more-efficient mNLRC4-mediated IL-1 $\beta$  activation (Fig. 3B and fig. S12B).

Wedging of Tyr<sup>617</sup> between the LRR domain and the NBD appears to be important for the interaction between the two domains (Fig. 3C). It stacks against His<sup>147</sup> from the NBD and forms an Asp<sup>615</sup>-mediated hydrogen bond with Tyr<sup>585</sup>, which in turn packs against Arg<sup>145</sup>. Supporting the structural observations, the mutant Y617A (Y, Tyr; A, Ala) constitutively activated IL-1 $\beta$  (Fig. 3D,

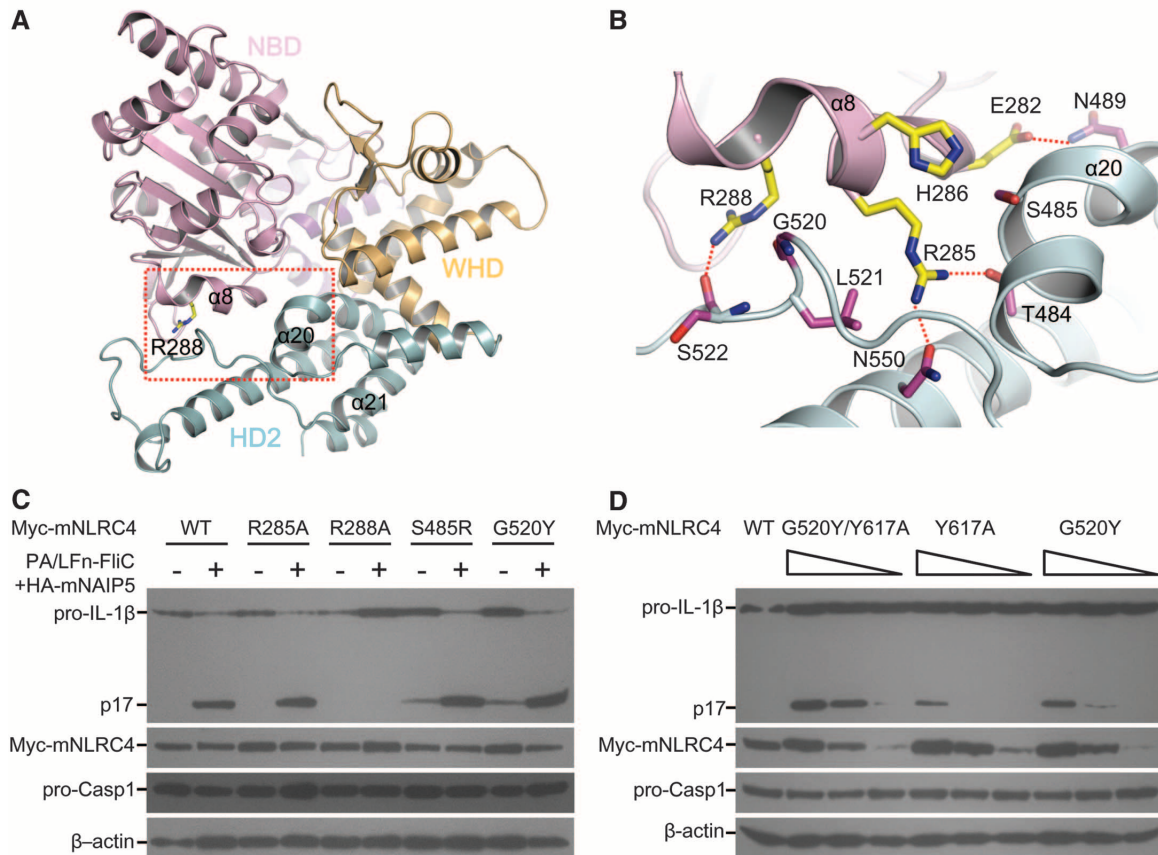


**Fig. 4. HD2 negatively regulates the function of a conserved  $\alpha$  helix from NBD.** (A) The  $\alpha 8$  helix from the NBD is occluded by HD2. Structural elements involved in the HD2-NBD interaction are labeled. (B) Detailed HD2-NBD interactions from the area highlighted in (A). The side chains from the NBD and the HD2 are shown in yellow and pink, respectively. E, Glu; T, Thr. (C) Analysis of mutants with disrupting HD2-NBD

interactions disrupted. The assay was performed as described in Fig. 2C and repeated for three times. (D) Analysis of a mNLRC4 variant with the HD2-NBD and LRR-NBD interactions disrupted. The assay was performed as described in Fig. 2C. A twofold serial dilution was made for the transfection of G520Y/Y617A, G520Y, and Y617A. The experiments were repeated three times.

fig. S13A and fig. S14). Consistent with its partially constitutive activity, the mutant was still responsive to flagellin (Fig. 3D).

HD2 exists in all NLRs (8), but whether and how it contributes to NLR autoinhibition remain unknown. The HD2 of mNLRC4ΔCARD is positioned differently from that of the inactive Apaf-1 (fig. S9) but similarly to the WHD of CED-4 that is involved in the formation of the CED-4 apoptosome (24) (fig. S11A). These structural observations suggest that HD2 may have a role in mNLRC4 autoinhibition. Consistent with this, the mNLRC4 mutant lacking HD2 and LRR domains was more efficient at activating IL-1 $\beta$  than the mutant lacking the LRR domain only (Fig. 3B). HD2 contacts  $\alpha$ 8 from NBD (Fig. 4, A and B), a conserved structural component involved in oligomerization of STAND family members (8, 21, 24). Mutation of Arg<sup>288</sup> but not Arg<sup>285</sup> of  $\alpha$ 8 to alanine abrogated flagellin-induced IL-1 $\beta$  activation (Fig. 4C and fig. S13C), supporting a critical role for  $\alpha$ 8 in mNLRC4 activation. Failure of the R288A (R, Arg) protein to activate IL-1 $\beta$  was not caused by its defect in folding or in interaction with mNAIP5 (fig. S15).

The NBD-HD2 interaction is mainly mediated by packing of  $\alpha$ 8 against  $\alpha$ 20 and the loop C-terminal to  $\alpha$ 21 (Fig. 4B). Ser<sup>485</sup> from  $\alpha$ 20 and Gly<sup>520</sup> from the loop act as supporting points for the packing, which is further strengthened by Arg<sup>285</sup> wedged between the loop and  $\alpha$ 20. The interactions with the HD2 domain result in steric masking of  $\alpha$ 8. As anticipated, the mutants S485R and G520Y (S, Ser; G, Gly) constitutively activated IL-1 $\beta$  (Fig. 4C, and figs. S13B and S14) but were still responsive to flagellin (Fig. 4C). The variant carrying the mutations of Y617A and G520Y became more efficient for ligand-independent IL-1 $\beta$  activation than either of the single mutants (Fig. 4D), suggesting a cooperative inhibition of mNLRC4 by the LRR and HD2 domains. Together, our data show that HD2 acts as an autoinhibitory domain by negatively regulating the function of the conserved  $\alpha$ 8 in mNLRC4 activation.

The effects generated by the mutation H443L (Fig. 2, C and D) demonstrate the important role of the His<sup>443</sup>-ADP interaction in NLRC4 autoinhibition. Given the conserved histidine (28) from other NLR proteins, some of the disease-related mutations (2–4) in the NLR proteins are expected to perturb a similar interaction and result in their constitutive activation. The LRR-mediated NLRC4 inhibition is reminiscent of CED-4 inhibition by CED-9 in which CED-9 blocks CED-4 oligomerization (25). In addition, the first WD40 domain in the inactive Apaf-1 overlaps with the LRR domain of mNLRC4 and an adjacent protomer of a lateral dimer from the Apaf-1 apoptosome (26) (fig. S16).

The close locations to a potential ligand-binding site (fig. S17A) make it possible for the HD2-NBD and the LRR-NBD interfaces to be perturbed upon ligand binding. The extensive WHD-HD2 (Fig. 1B) and HD2-LRR interactions (fig. S8) appear not sufficiently labile to be disrupted to allow substantial conformational changes

in one domain with respect to the other two. Additionally, phosphorylation of Ser<sup>533</sup> (pS533) (fig. S18), which is critical for assembly of the mNLRC4 inflammasome (15), acts to stabilize the HD2-LRR interaction. Thus, ligand binding may disengage the three domains as a whole from the NBD, rendering it accessible to a second NLRC4 molecule for oligomerization (fig. S17B). pS533 can have a role in this process through unknown mechanisms. Regardless of the mechanism of intermediates, it seems that ligand binding allosterically activates the assembly of the NLRC4 inflammasome.

#### References and Notes

1. J. von Moltke, J. S. Ayres, E. M. Kofoed, J. Chavarría-Smith, R. E. Vance, *Annu. Rev. Immunol.* **31**, 73 (2013).
2. L. Franchi, R. Muñoz-Planillo, G. Núñez, *Nat. Immunol.* **13**, 325 (2012).
3. V. A. Rathinam, S. K. Vanaja, K. A. Fitzgerald, *Nat. Immunol.* **13**, 333 (2012).
4. T. M. Ng, J. Kortmann, M. D. Monack, *Curr. Opin. Immunol.* **25**, 34 (2013).
5. T. Strowig, J. Henao-Mejia, E. Elinav, R. Flavell, *Nature* **481**, 278 (2012).
6. H. Wen, J. P. Ting, L. A. O'Neill, *Nat. Immunol.* **13**, 352 (2012).
7. L. Zitvogel, O. Kepp, L. Galluzzi, G. Kroemer, *Nat. Immunol.* **13**, 343 (2012).
8. O. Danot, E. Marquet, D. Vidal-Ingigliardi, E. Richet, *Structure* **17**, 172 (2009).
9. F. Martinon, K. Burns, J. Tschopp, *Mol. Cell* **10**, 417 (2002).
10. B. Faustin *et al.*, *Mol. Cell* **25**, 713 (2007).
11. J. A. Duncan *et al.*, *Proc. Natl. Acad. Sci. U.S.A.* **104**, 8041 (2007).
12. J. L. Poyet *et al.*, *J. Biol. Chem.* **276**, 28309 (2001).
13. E. F. Halff *et al.*, *J. Biol. Chem.* **287**, 38460 (2012).
14. E. M. Kofoed, R. E. Vance, *Nature* **477**, 592 (2011).
15. Y. Qu *et al.*, *Nature* **490**, 539 (2012).

16. L. Franchi *et al.*, *Nat. Immunol.* **7**, 576 (2006).
17. E. A. Miao *et al.*, *Nat. Immunol.* **7**, 569 (2006).
18. A. B. Molofsky *et al.*, *J. Exp. Med.* **203**, 1093 (2006).
19. Y. Zhao *et al.*, *Nature* **477**, 596 (2011).
20. E. A. Miao *et al.*, *Proc. Natl. Acad. Sci. U.S.A.* **107**, 3076 (2010).
21. J. P. Erzberger, J. M. Berger, *Annu. Rev. Biophys. Biomol. Struct.* **35**, 93 (2006).
22. S. J. Riedl, W. Li, Y. Chao, R. Schwarzenbacher, Y. Shi, *Nature* **434**, 926 (2005).
23. T. F. Reubold, S. Wohlgemuth, S. Eschenburg, *Structure* **19**, 1074 (2011).
24. S. Qi *et al.*, *Cell* **141**, 446 (2010).
25. N. Yan *et al.*, *Nature* **437**, 831 (2005).
26. S. Yuan, M. Topf, T. F. Reubold, S. Eschenburg, C. W. Akey, *Biochemistry* **52**, 2319 (2013).
27. S. Yuan *et al.*, *Structure* **19**, 128 (2011).
28. M. Proell, S. J. Riedl, J. H. Fritz, A. M. Rojas, R. Schwarzenbacher, *PLoS ONE* **3**, e2119 (2008).

**Acknowledgments:** We thank P. Schulze-Lefert for critically reading the manuscript, F. Yu and J. He at Shanghai Synchrotron Radiation Facility BL17U1 for data collection, L. Yu for helpful suggestions on culturing 293T cells, G. He from Y. Yan's laboratory assistance with CD, and J. Yang from F. Shao's laboratory for suggestions on cell-based assays. The coordinates and structural factors for mNLRC4ΔCARD have been deposited in the Protein Data Bank (PDB) with the accession code 4KXF. This research was funded by the National Outstanding Young Scholar Science Foundation of China (20101331722) and State Key Program of National Natural Science of China (31130063) to J. Chai.

#### Supplementary Materials

www.sciencemag.org/cgi/content/full/science.1236381/DC1  
Materials and Methods  
Figs. S1 to S18  
Table S1  
References (29–39)

11 February 2013; accepted 30 May 2013  
Published online 13 June 2013;  
10.1126/science.1236381

## Biosynthesis of Antinutritional Alkaloids in Solanaceous Crops Is Mediated by Clustered Genes

M. Itkin,<sup>1\*</sup> U. Heinig,<sup>1</sup> O. Tzfadia,<sup>1</sup> A. J. Bhide,<sup>1,2</sup> B. Shinde,<sup>1,2</sup> P. D. Cardenas,<sup>1</sup> S. E. Bocobza,<sup>1</sup> T. Unger,<sup>4</sup> S. Malitsky,<sup>1</sup> R. Finkers,<sup>5</sup> Y. Tikunov,<sup>5</sup> A. Bovy,<sup>5</sup> Y. Chikate,<sup>1,2</sup> P. Singh,<sup>1,2</sup> I. Rogachev,<sup>1</sup> J. Beekwilder,<sup>5</sup> A. P. Giri,<sup>1,2</sup> A. Aharoni<sup>1†</sup>

Steroidal glycoalkaloids (SGAs) such as  $\alpha$ -solanine found in solanaceous food plants—as, for example, potato—are antinutritional factors for humans. Comparative coexpression analysis between tomato and potato coupled with chemical profiling revealed an array of 10 genes that partake in SGA biosynthesis. We discovered that six of them exist as a cluster on chromosome 7, whereas an additional two are adjacent in a duplicated genomic region on chromosome 12. Following systematic functional analysis, we suggest a revised SGA biosynthetic pathway starting from cholesterol up to the tetrasaccharide moiety linked to the tomato SGA aglycone. Silencing *GLYCOALKALOID METABOLISM 4* prevented accumulation of SGAs in potato tubers and tomato fruit. This may provide a means for removal of unsafe, antinutritional substances present in these widely used food crops.

**O**ur demand for more and better food continues to increase. Improved nutritional qualities, as well as removal of antinutritional traits, are needed. Various approaches have been used to add nutritional qualities to food crops. We focus here on reducing the level of endogenous, antinutritional factors in existing crops (1). Anti-

nutritional substances range from lethal toxins to compounds that disrupt digestion and nutrient absorption (2). In the course of crop domestication, levels of antinutrients were reduced by selection and/or breeding, although some of such substances remain in the general food source. In addition, wild germplasm, which can be useful as a source of

## Crystal Structure of NLRC4 Reveals Its Autoinhibition Mechanism

Zehan Hu, Chuangye Yan, Peiyuan Liu, Zhiwei Huang, Rui Ma, Chenlu Zhang, Ruiyong Wang, Yueteng Zhang, Fabio Martinon, Di Miao, Haiteng Deng, Jiawei Wang, Junbiao Chang and Jijie Chai

*Science* **341** (6142), 172-175.  
DOI: 10.1126/science.1236381 originally published online June 13, 2013

### Keeping the Inflammasome in Check

Nucleotide-binding and oligomerization domain (NOD)-like receptors (NLRs) play an important role in the detection of pathogens by cells of the innate immune system. For several NLR family members, activation results in relief from autoinhibition, oligomerization, and the recruitment of signaling components that together make up the inflammasome, a large multiprotein complex. The inflammasome protects the host by inducing cell death and cytokine secretion. The specific molecular mechanisms that regulate NLR activation and inhibition, however, are not well understood. **Hu *et al.*** (p. 172, published online 13 June) report the crystal structure of autoinhibited NLR family member NLRC4, which reveals the domains that are critical for interaction with adenosine diphosphate to keep NLRC4 in its inactive state and the domains that mediate oligomerization of the protein upon activation.

#### ARTICLE TOOLS

<http://science.sciencemag.org/content/341/6142/172>

#### SUPPLEMENTARY MATERIALS

<http://science.sciencemag.org/content/suppl/2013/06/12/science.1236381.DC1>

#### RELATED CONTENT

<http://stke.sciencemag.org/content/sigtrans/6/284/ec164.abstract>

#### REFERENCES

This article cites 39 articles, 7 of which you can access for free  
<http://science.sciencemag.org/content/341/6142/172#BIBL>

#### PERMISSIONS

<http://www.sciencemag.org/help/reprints-and-permissions>

Use of this article is subject to the [Terms of Service](#)